



# Microfabric study on the deformational and thermal history of the Alpi Apuane marbles (Carrara marbles), Italy

G. Molli<sup>a,\*</sup>, P. Conti<sup>b</sup>, G. Giorgetti<sup>b</sup>, M. Meccheri<sup>b</sup>, N. Oesterling<sup>c</sup>

<sup>a</sup>*Dipartimento di Scienze della Terra, Università di Pisa and C.N.R. Centro di Studio Geologia Strutturale e Dinamica App.Sett., Via S.Maria 53, I-56126 Pisa, Italy*

<sup>b</sup>*Dipartimento di Scienze della Terra, Università di Siena, Via Laterina 8, I-53100 Siena, Italy*

<sup>c</sup>*Department of Earth Sciences, University of Basel, Bernoullistr. 32, CH-4056 Basel, Switzerland*

Received 30 November 1999; accepted 26 June 2000

## Abstract

Marbles from different geometrical and structural positions within the Alpi Apuane metamorphic complex show a large variability in microfabric types as indicated by microstructure, *c*-axis orientation and temperature analysis.

Statically recrystallized samples showing a granoblastic microstructure and polygonal grain boundaries are characterized by a grain size variation from east to west from 80–100  $\mu\text{m}$  to 250–300  $\mu\text{m}$ . This is correlated with an equilibration calcite-dolomite temperature from 360–380°C to 420–430°C.

Two kinds of dynamically recrystallized microstructures have been investigated: a first one exhibiting coarse grains (150–200  $\mu\text{m}$ ) with lobate grain boundaries and a strong shape preferred orientation and a second one characterized by a smaller grain size (40–50  $\mu\text{m}$ ) and predominantly straight grain boundaries. These microstructural types, associated with localized post-thermal peak shear zones and meter- to kilometer-scale folds, are interpreted as related to high strain and high temperature crystal plastic deformation mechanisms (dislocation creep) associated with predominant grain boundary migration (type-B1) or subgrain-rotation recrystallization (type-B2). These differences in dynamically recrystallized microstructures are related to equilibration temperatures higher in type-B1 (390°C) than in type-B2 (370–340°C). We have been able to relate the development of the different microfabric types to the successive stages of deformation of the Alpi Apuane metamorphic complex. © 2000 Elsevier Science Ltd. All rights reserved.

## 1. Introduction

The marbles from the Alpi Apuane, and in particular the white variety called “Carrara marble”, are well known geological materials due to their extensive use both as building stones and for statuary as well as in rock-deformation experiments (Rutter, 1972; Casey et al., 1978; Spiers, 1979; Schmid et al., 1980; Schmid et al., 1987; Wenk et al., 1987; Fredrich et al., 1989; De Bresser, 1991; Rutter, 1995; Covey-Crump, 1997). In the latter, Carrara marble is widely used because: a) it is an almost pure calcite marble; b) it shows a nearly homogenous fabric, with no or weak grain-shape or crystallographic preferred orientation; c) it usually develops a large grain-size; and d) a large amount of literature data about its behaviour under various experimental deformation conditions is available.

All the above features can be found in large volumes of marbles cropping out in the Carrara area, i.e. in the north-

western part of the Alpi Apuane region (Fig. 1), but are not common in marbles from other areas of the Alpi Apuane. In this paper, we illustrate the main fabric types we have recognized in marbles from the Alpi Apuane area and discuss fabric development, taking into account the role of the regional deformation history and the position of marbles in kilometer- to meter-scale geological structures. To exclude the influence of second phase particles like phyllosilicates on the microfabric development (Olgaard and Evans, 1988; Mas and Crowley, 1996), we have concentrated on the pure white calcite marbles.

In the following, “Alpi Apuane marbles” indicates the Liassic marble formation cropping out in the whole Alpi Apuane area, while “Carrara marble” stands for marbles located in the northwestern Alpi Apuane area in the surroundings of the town of Carrara (Fig. 1). Carrara marbles are the most intensely quarried marble variety within the entire Alpi Apuane. Due to their economic and cultural importance, Alpi Apuane marbles have been the object of geological investigation for a century (Zaccagna, 1932; Bonatti, 1938), with general studies

\* Corresponding author.

E-mail address: gmolli@dst.unipi.it (G. Molli).

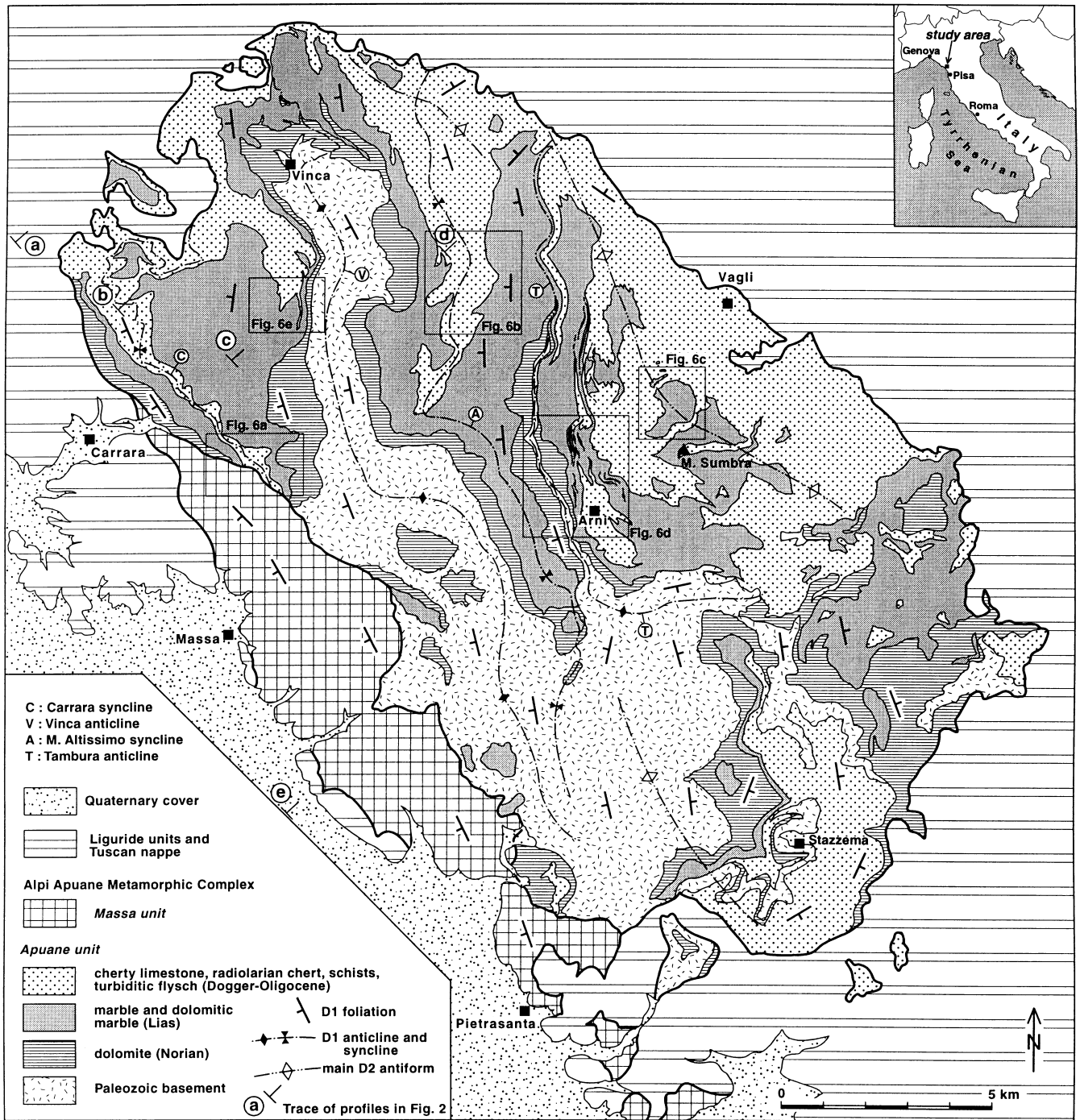


Fig. 1. Structural map of the Alpi Apuane area (from Carmignani et al., 1978, 1993, modified). See Fig. 2 for cross-sections. Locations of detailed geological maps of Fig. 6 are indicated.

appearing in the sixties and seventies (D'Albissin, 1963; Crisci et al., 1975; Di Sabatino et al., 1977). Di Pisa et al. (1985) were the first who presented calcite/dolomite thermometric estimates within the general tectonic evolution of the Alpi Apuane metamorphic complex. Later on, Coli (1989) focused on marbles from the microstructural point of view, providing a qualitative and general descrip-

tion of some microstructures. A more recent contribution by Coli and Fazzuoli (1992) tackled the problem of the Alpi Apuane marble from a lithostratigraphic point of view.

The aim of our study is to describe microfabric types in different geometrical positions in the polyphase nappe building of the Alpi Apuane metamorphic complex and

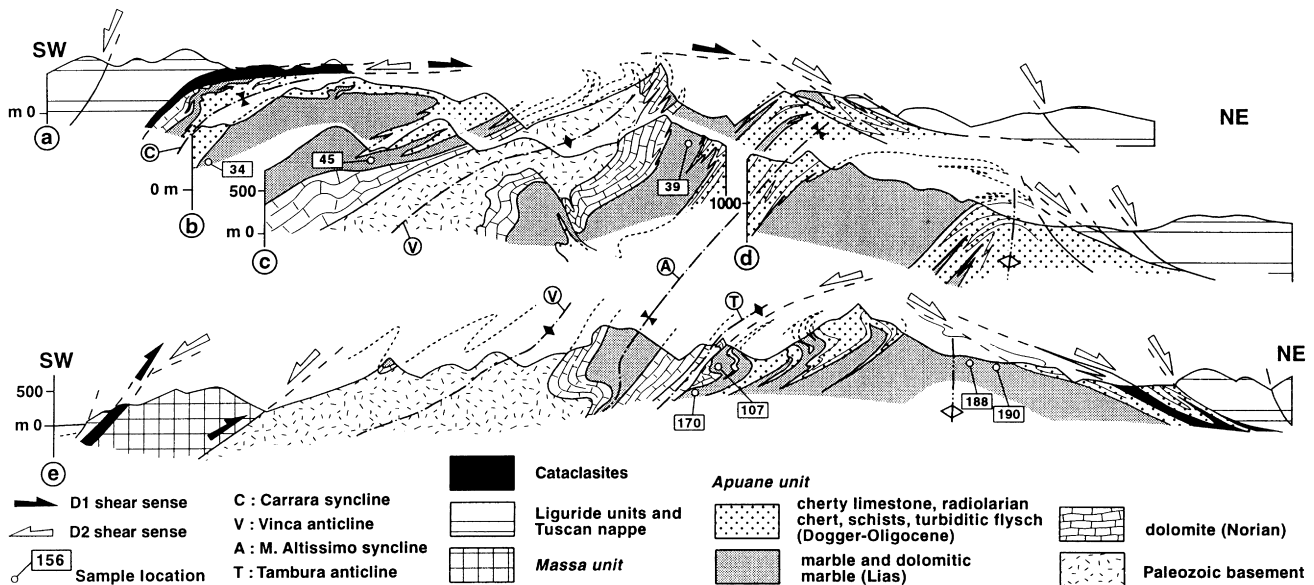


Fig. 2. Composite cross-sections in the Alpi Apuane area (from Carmignani et al., 1993).

their relationship with large- to small-scale tectonic structures. Structural data are supplemented by a calcite/dolomite investigation to constrain the thermal conditions for each microfabric type formation.

## 2. Geological setting

The lowermost tectonic units of the northern Apennine fold-and-thrust belt are exposed in the Alpi Apuane region (Figs. 1 and 2). According to classical interpretations (Elter, 1975; Carmignani et al., 1978, and reference therein), the following units can be recognized in this area from top to bottom.

1. The Liguride units, formed by ophiolites and deep-water sediments, representing the Mesozoic Ligurian ocean and parts of an accretionary wedge system related to the closure of the ocean itself. These units show anchimetamorphic to very low grade metamorphic conditions (Cerrina et al., 1983; Reutter et al., 1983).
2. The sub-Liguride unit (Canetolo unit), corresponding to part of the sedimentary cover of the ocean–continent transitional area.
3. The Tuscan nappe, a continent-derived unit formed by a Late Triassic to Aquitanian sedimentary sequence, deposited on the Apulia domain, detached from its original basement and characterized by a polyphase deformation associated with a very low grade metamorphism.
4. The Massa unit, with a pre-Mesozoic basement and a well developed Middle to Late Triassic sequence, associated with Middle Triassic metavolcanic rocks, deformed and metamorphosed in greenschist facies conditions.

5. The lowermost Apuane unit, made up by a Hercynian basement unconformably overlain by Triassic to Oligocene greenschist facies metamorphic rocks. The Mesozoic-tertiary succession in this unit is characterized by Triassic dolomite turning to Liassic marble and dolomitic marble. The succession (Dogger to Oligocene) continues with cherty limestones, radiolarian chert, schist, and turbiditic flysch.

In the Alpi Apuane, marbles derive from stratigraphically different levels. They are of Devonian, as well as of Liassic, Dogger and Cretaceous–Eocene age. We have focussed our attention on the Liassic marbles, which belong to the thickest and purest succession.

The northern Apennine is derived from the westernmost sector of the Apulia continental margin in the Late Jurassic paleogeography. Deformation started during Eocene times, first affecting the inner and originally westernmost domains (Liguride and sub-Liguride units), and then continuing in the Late Oligocene–Miocene to involve the more external Tuscan domain (Tuscan nappe, Massa unit and Apuane unit). Northeastward facing folding and northeastward nappe transport occurred throughout, resulting in a thick nappe stack development. Starting in the Early Miocene, contraction shifted toward more external (i.e. Umbria–Marchean) domains and the internal northern Apennines suffered extensional tectonics with uplift and tectonic denudation. In the Late Miocene the regional extensional tectonics related to the opening of the Tyrrhenian Sea affected the area (e.g. Carmignani and Kligfield, 1990; Storti, 1995 and reference therein).

In the Massa unit and the Apuane unit, two main polyphase tectono-metamorphic events can be recognized, the  $D_1$  and  $D_2$  events (Carmignani and Kligfield, 1990). During

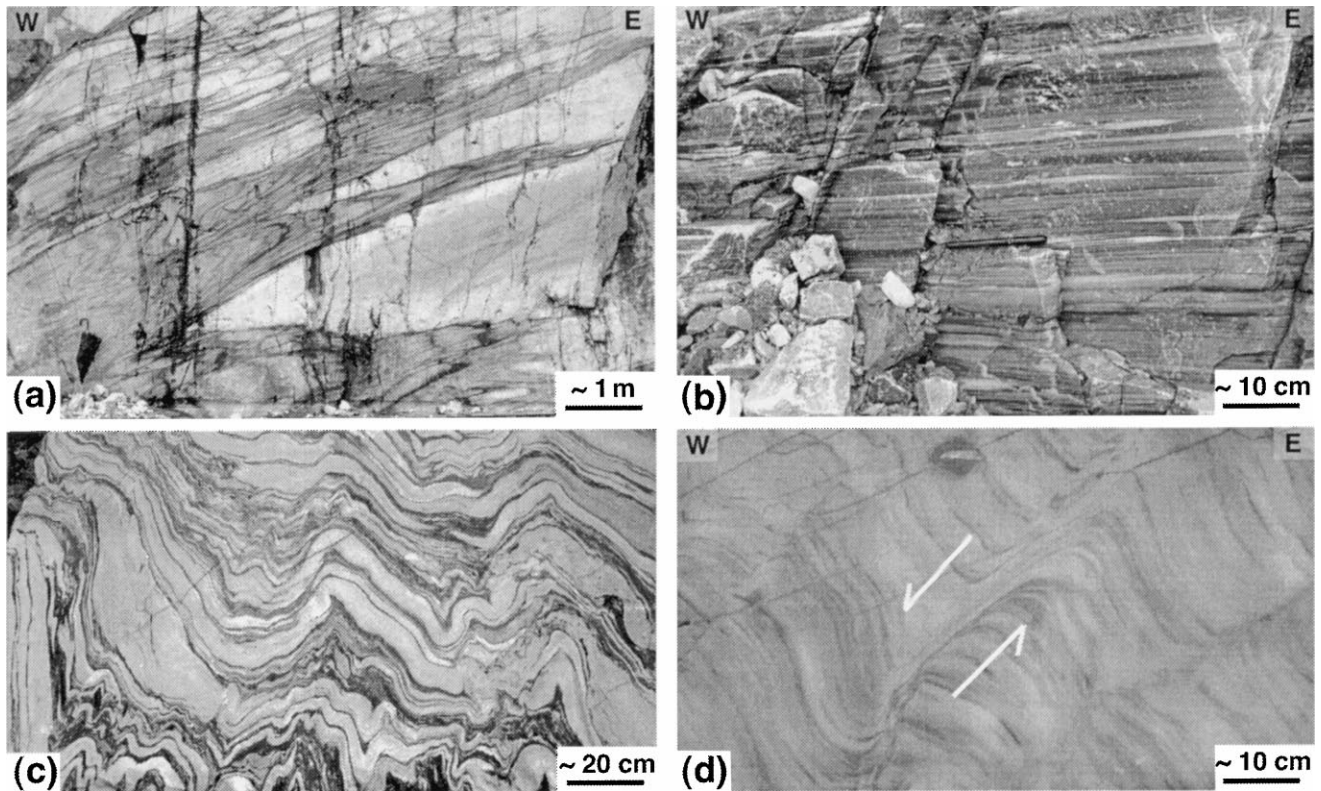


Fig. 3. (a)  $D_1$  isoclinal folds in marbles (Vallini quarry, western Alpi Apuane). (b)  $D_1$  shear zone in cherty limestones (Vallini, western Alpi Apuane). (c)  $D_2$  folds refolding main foliation in marble breccia (Arni, central Alpi Apuane). (d)  $D_2$  shear zones cutting  $D_1$  foliation in marbles (Arni, central Alpi Apuane).

$D_1$ , nappe emplacement occurred, with development of kilometer-scale NE facing isoclinal folds (Fig. 3a), NE–SW oriented stretching lineations ( $L_1$ ) and a greenschist facies ubiquitous regional foliation ( $S_1$ ). In more detail, the  $D_1$  event can be subdivided into: a) a “main folding phase”, in which kilometer-scale recumbent folds and an associated flat-lying axial plane foliation are formed; b) an “antiformal stack phase”, in which final nappe emplacement occurred, together with antiformal stack development and formation of shear zones (Fig. 3b). Shear zones show again top-to-the-NE/E sense of movement.

The  $D_2$  event deforms all earlier features, developing folds (Fig. 3c) and shear zones (Fig. 3d), leading to progressive unroofing and exhumation of the metamorphic complex at higher structural levels.  $D_2$  is characterized by retrograde metamorphic conditions and the latest stages of deformation are associated with polyphase brittle structures.

Greenschist facies conditions were achieved in the Apuane unit during  $D_1$  and early  $D_2$  deformation (Carmignani et al., 1978). The occurrence of the stable association pyrophyllite + quartz (Franceschelli et al., 1986, 1997) indicates temperatures between 300–450°C and pressure ranging from 0.5–0.6 GPa (Di Pisa et al., 1985; Schultz, 1996; Franceschelli et al., 1997) and 0.6–0.8 GPa (Jolivet et al., 1998). Peak of metamorphic conditions yielding to annealing was attained during the main deformational event ( $D_1$ ) and before the  $D_2$  event (Bocca-

letti and Gosso, 1980; Carmignani and Kligfield, 1990; Franceschelli et al., 1997; Molli and Giorgetti, 1999).

Radiometric K/Ar and  $^{40}\text{Ar}/^{39}\text{Ar}$  data suggest that  $D_1$  occurred approximately at 27 Ma and that early  $D_2$  deformation ended at 10–8 Ma (Giglia and Radicati di Brozolo, 1970; Kligfield et al., 1986). Cooling through 100–120°C temperature can be constrained by fission tracks data ranging from 6 to 2 Ma (Bigazzi et al., 1988; Abbate et al., 1994).

### 3. Studied samples and analytical techniques

The samples analysed were collected in different geometrical positions in the Apuane unit (Figs. 1 and 2) along a SW–NE oriented transection parallel to the  $D_1$  transport direction. Marbles are quite homogeneous, being composed of more than 99% of calcite, plus minor contributions of quartz, albite, white mica and/or opaque minerals, as confirmed by chemical analyses of major and minor elements (Table 1).

All samples were cut parallel to the stretching lineation  $L_1$  and normal to the foliation plane  $S_1$ . Ultra-thin sections (<4  $\mu\text{m}$  thick) were prepared and analysed by optical microscopy. To quantify the grain shapes, quantitative microstructural analyses were performed using preferred orientations of the particle axes (PAROR) (Fig. 4a) and

Table 1  
Whole-rock chemical analyses of a typical “granoblastic” annealed marble (Type A) and of a typical dynamically recrystallized marble (Type B). Composition was obtained using a XRF spectrometer Philips PW1414

Wt% Oxide	Type A	Type B
SiO <sub>2</sub>	0.15	0.05
TiO <sub>2</sub>	-	-
Al <sub>2</sub> O <sub>3</sub>	0.08	0.09
Fe <sub>2</sub> O <sub>3</sub>	0.12	0.11
FeO	-	-
MgO	1.08	1.24
MnO	-	-
CaO	54.92	54.66
Na <sub>2</sub> O	-	-
K <sub>2</sub> O	-	-
P <sub>2</sub> O <sub>5</sub>	0.11	0.12
L.O.I.	43.50	43.70

symmetry of the orientation of the grain boundary surfaces (SURFOR) (Fig. 4b) methods (Panozzo, 1983, 1984). Grain boundary corrugation was determined using the SHAPES program (Panozzo and Hürlimann, 1983) and characterized with the PARIS factor (Panozzo and Hürlimann, 1983, see Fig. 4c), which takes into account the convexity–concavity of the grain boundary geometry.

In order to characterize the crystallographic preferred orientation (CPO, texture), universal stage measurements as well as computer integrated polarization microscopy (CIP) (Heilbronner Panozzo and Pauli, 1993) were carried out. The latter method uses the interference colour of each pixel of a series of digitally recorded thin-section images for the determination of the *c*-axis orientation. Basically, the CIP-method is similar to the “Achsenverteilunganalyse” (AVA) of Sander (1950), where the thin-section image is colour coded according to its *c*-axis orientation and a certain stereographic colour look-up table (CLUT).

The interference colour of optically uniaxial minerals is a function of the thin-section thickness and the birefringence as well as a function of the *c*-axis orientation. By the variation of the thin-section thickness, the effect of the birefringence on the interference colour can be controlled, e.g. lowering the thin-section thickness provides an interference colour. Therefore the *c*-axis orientation can be directly determined by the interference colour. The CIP-method requires interference colours of first-order grey. Since calcite has a high birefringence (0.172), thin-sections of about <2 μm thickness had to be prepared.

Dolomite-bearing marbles were carefully investigated in order to constrain the equilibrium temperatures of different calcite-dolomite relations. Calcite and dolomite grains were analyzed by wavelength-dispersive spectrometry using a Jeol JXA 8600 microprobe operating at 15 kV and 10 nA. Analyzed elements included Ca, Mg, Mn, Fe, Sr, Ba with count times of 15 s for Ca and 30 s for all the other elements. A defocused beam (up to 10 μm) was used to avoid volatilization and reintegration of possible submicroscopic exsolution of dolomite lamellae. Chemical resetting occurs easily in carbonates during retrogression and either magnesian calcite grains may exsolve dolomite lamellae or the original high Mg content is obliterated by intracrystalline diffusion (Essene, 1982). Consequently, retrograde re-equilibration produces calcite grains with Mg content lower than that attained at peak metamorphic conditions. All samples show grain-to-grain variations in Mg content, even among calcite grains with the same microstructural features and such variations are attributed to retrograde resetting (Essene, 1989). For this reason, averaging the data would obliterate this effect leading to underestimation of the peak temperature. Therefore, we consider the maximum Mg content recorded in each calcite microstructural type to calculate the actual

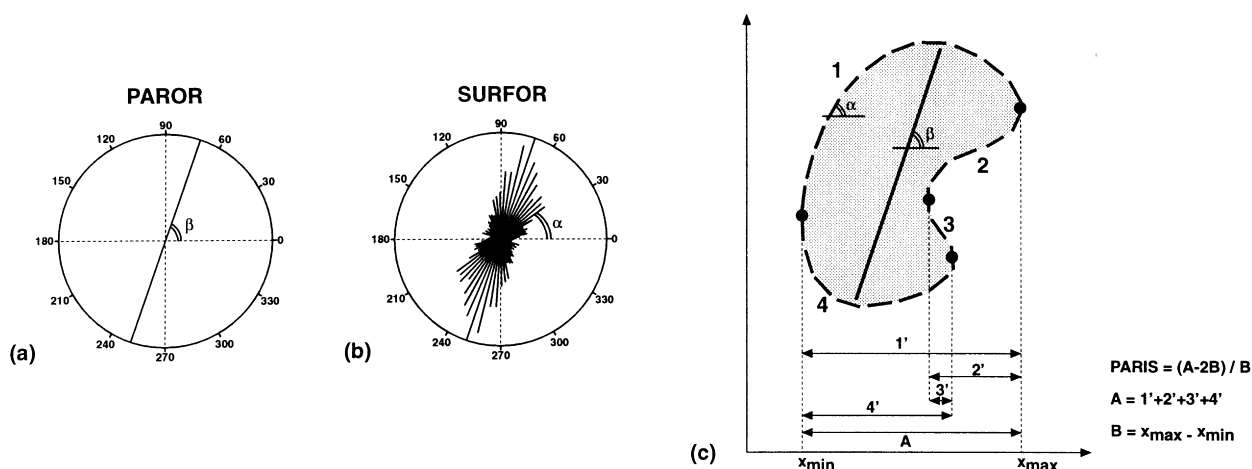


Fig. 4. Schematic illustration of the image analysis by means of PAROR and SURFOR method (for more details see Panozzo, 1983, 1984; Panozzo and Hürlimann, 1983). Each grain boundary is digitized and consists of short line segments. (a) Using projection method the PAROR routine presents in a rose diagram the general orientation of the grains ( $\beta$ ) with respect to a reference line (in this study the foliation trace). (b) The SURFOR routine, using projection methods, presents the cumulative orientation of the line segments in a rose diagram;  $\alpha$  is the orientation of the line segment with respect to a reference line. (c) The PARIS factor gives quantitative indication of corrugation of the grain boundaries and increases with migration of grain boundary.

Table 2

Chemical analyses of calcite grains; all formulae normalized to two cations per formula unit. Temperatures calculated using Anovitz and Essene (1987) calibration. A refers to granoblastic calcite grains; B refers to recrystallized calcite grains; c: core composition; r: rim composition

	Sample n.										
	30	40	4	188	115	107A	107Bc	107Br	45Ac	45Ar	45B
<i>Wt. % Oxide</i>											
CaO	55.15	54.02	53.78	55.15	54.71	54.30	53.72	54.65	53.84	54.49	54.48
MgO	1.25	0.92	0.92	0.85	0.97	1.09	1.01	0.91	0.95	0.87	0.78
FeO	0.03	0.02	0.00	0.02	0.05	0.00	0.04	0.04	0.04	0.04	0.02
MnO	0.06	0.3	0.05	0.04	0.05	0.00	0.07	0.00	0.00	0.01	0.00
SrO	0.26	0.15	0.03	0.09	0.04	0.04	0.00	0.00	0.10	0.05	0.03
BaO	0.00	0.00	0.00	0.00	0.02	0.03	0.00	0.00	0.00	0.03	0.00
Sum	56.75	55.14	54.78	56.15	55.84	55.46	54.84	55.60	54.93	55.49	55.31
CO <sub>2</sub>	44.81	43.49	43.25	44.29	44.08	43.83	43.33	43.91	43.35	43.78	43.63
Total	101.56	98.62	98.03	100.44	99.93	99.29	98.17	99.51	98.28	99.27	98.94
<i>No. of ions</i>											
Ca	1.93	1.95	1.95	1.95	1.95	1.94	1.95	1.95	1.95	1.95	1.96
mg	0.06	0.046	0.05	0.04	0.05	0.05	0.05	0.05	0.05	0.04	0.04
Fe	0.00	0.001	0.00	0.00	0.00	0.00	0.00	0.00	0.00	0.00	0.00
Mn	0.00	0.001	0.00	0.00	0.00	0.00	0.00	0.00	0.00	0.00	0.00
Sr	0.01	0.003	0.00	0.00	0.00	0.00	0.00	0.00	0.00	0.00	0.00
Ba	0.00	0.00	0.00	0.00	0.00	0.00	0.00	0.00	0.00	0.00	0.00
<i>Mol. %</i>											
CaCO <sub>3</sub>	98.42	96.41	95.99	98.44	97.65	96.91	95.87	97.54	96.09	97.25	97.24
MgCO <sub>3</sub>	2.61	1.92	1.92	1.78	2.03	2.28	2.11	1.91	1.98	1.82	1.63
FeCO <sub>3</sub>	0.06	0.03	0.00	0.04	0.08	0.00	0.06	0.07	0.07	0.07	0.03
MnCO <sub>3</sub>	0.10	0.05	0.08	0.06	0.09	0.00	0.12	0.00	0.00	0.02	0.00
SrCO <sub>3</sub>	0.38	0.21	0.05	0.18	0.05	0.06	0.00	0.00	0.14	0.07	0.05
BaCO <sub>3</sub>	0.00	0.00	0.00	0.00	0.02	0.03	0.00	0.00	0.00	0.04	0.00
T°C	433	380	377	360	388	409	399	375	390	360	346

maximum metamorphic conditions (Essene, 1983). The reported temperatures (Table 2) were calculated using the calcite-dolomite thermometer calibrated by Anovitz and Essene (1987) which accounts for Fe in the system. The position of the solvus is well defined between 400 and 800°C with an error in the estimations of  $\pm 10^\circ\text{C}$ ; below 400°C the solvus limb steepens and potential errors increase (Anovitz and Essene, 1987). However, even at low temperature, consistency in the relative variations in the Mg content is significant. In this case, temperatures lower than 400°C are affected by large errors, but reflect an actual trending in temperature variation.

#### 4. Microfabrics of the Alpi Apuane marbles

Microstructural features, allow us to distinguish three main types of microfabrics in the Alpi Apuane marbles. They represent end-members of a wide range of transitional types. Each microfabric type can be found in the whole Alpi Apuane area. The three main microfabric types are: a) annealed microfabric (type-A); b) dynamically recrystallized microfabric (type-B) and c) twinned microfabric (type-C).

##### 4.1. Annealed microfabric (type-A microfabric)

This type of microfabric is characterized by equant polygonal grains (granoblastic or “foam” microstructure, Fig. 5 a–d), with straight to slightly curved grain boundaries that meet in triple points at angles of nearly  $120^\circ$ . *c*-Axis orientations show a random distribution or a weak crystallographic preferred orientation. Samples showing this microstructure come from different structural and geographical positions in the Alpi Apuane unit: sample 34 from the western, sample 39 from the central and sample 190 from the eastern Alpi Apuane (Fig. 2).

The westernmost sample (sample 34) is located in the normal limb of a regional scale NE-facing D1 isoclinal fold, the Carrara syncline (Figs. 2 and 6a). This kilometer-scale syncline represents the major westernmost fold in the Apuane unit with a NW–SE trending axis, shallowly plunging to the NW. Microstructural analysis of this sample shows a unimodal grain size distribution with an average grain size of 300  $\mu\text{m}$  (Molli and Heilbronner, 1999). The analysis of the preferred orientation of grain boundary surfaces (SURFOR) reveals a slightly bimodal surface distribution which can be observed in the rose diagram of Fig. 7a. This may reflect a weak grain boundary alignment

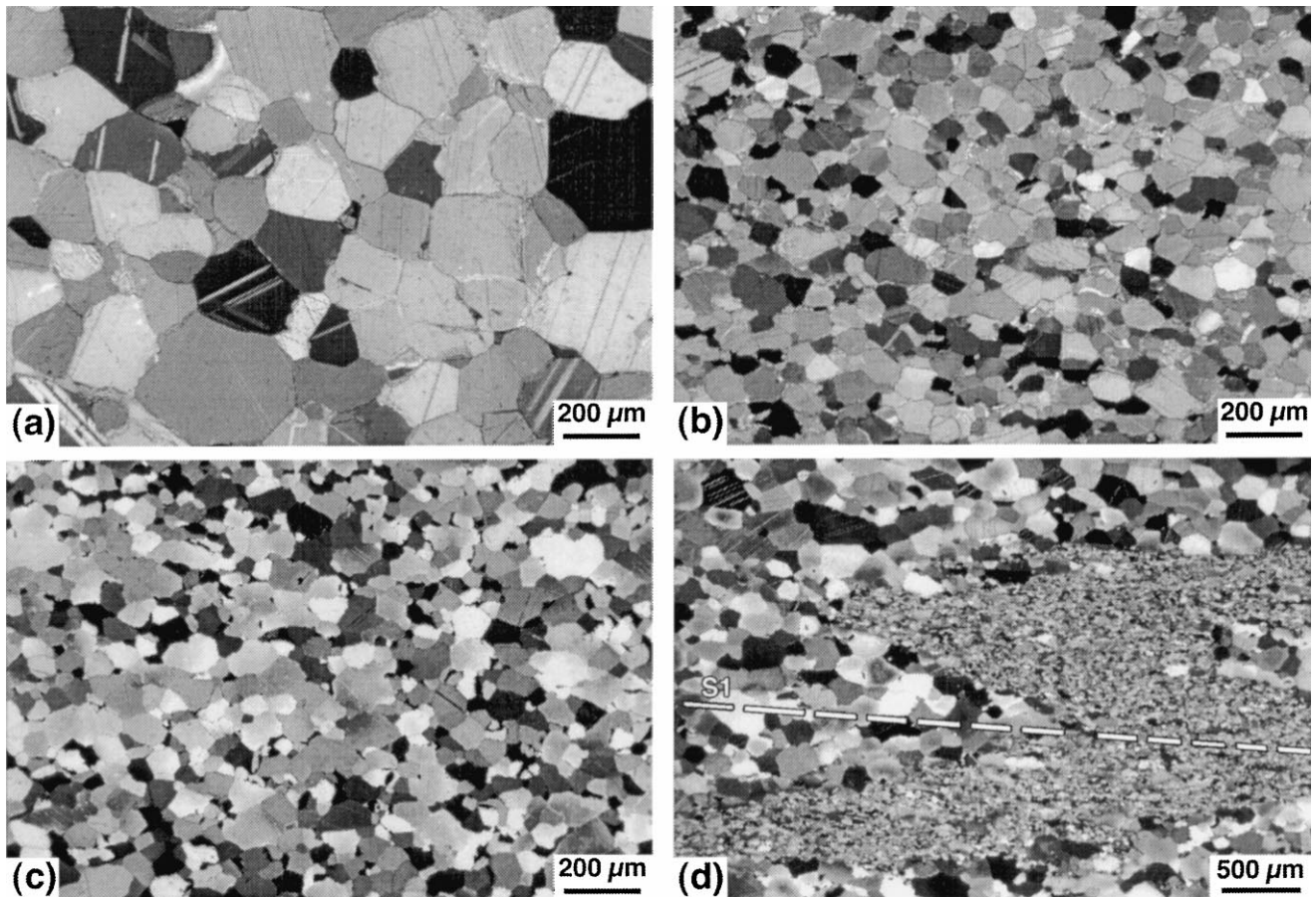


Fig. 5. Annealed microstructures in marbles: (a) Sample 34. (b) Sample 39. (c) Sample 180. (d)  $D_1$  fold overgrown by “granoblastic” microstructure (locality Belgium, western Alpi Apuane). The folded level, made up of fine-grained, calcite dolomite and phyllosilicates, represents a former stratigraphic layer.

of rhombic symmetry, which has been already noticed for undeformed marble before (Schmid et al., 1987). The analysis of the preferred orientation of particle axes (PAROR) also shows a slightly bimodal distribution of long axis orientation, with the first maximum being inclined at approximately  $20\text{--}30^\circ$  with respect to the foliation plane, and a second maximum at  $20\text{--}30^\circ$  in the opposite sense (Table 3). The asymmetry of the orientation of grain boundary surfaces (SURFOR) and the preferred orientations of the particle axes (PAROR) of the sample coincide rather well. The average aspect ratios (short/long axis) of the individual grains are in the order of 0.65. The PARIS factor for this microstructure is very low (1.8), implying straight grain boundaries. The  $c$ -axis pole figure reveals a weak great circle distribution at the periphery of the pole figure. The maximum temperature calculated for a dolomite-bearing sample collected in the same outcrop (sample 30) is about  $430^\circ\text{C}$  (Table 2).

Sample 39 comes from the central-northern part of the Alpi Apuane, in the normal limb of the M. Altissimo Syncline (Fig. 6b). The quantitative microstructural analysis of sample 39 shows a unimodal grain size distribution with an average grain size diameter of  $90\ \mu\text{m}$  (Molli and Heilbronner, 1999) (Fig. 7b). A unimodal and asymmetrical

surface orientation is revealed by the analysis of the preferred orientation of grain boundary surfaces (SURFOR) showing a maximum of orientation at an angle of approximately  $30^\circ$  to the foliation trace. The analysis of the preferred orientation of particle axes (PAROR) shows a weak bimodal distribution of long axis orientation, with the first maximum being inclined at approximately  $20\text{--}30^\circ$  with respect to the foliation plane, and a second maximum at  $20\text{--}30^\circ$  in the opposite sense. Also in this sample the symmetry of the orientation of grain boundary surfaces (SURFOR) and the preferred orientations of the particle axes (PAROR) coincide rather well. The average aspect ratios (short/long axis) of the individual grains are in the order of 0.65 and the PARIS factor of microstructures is 2.3. Sample 39 shows a nearly random distribution of  $c$ -axis. Samples 40 and 4, collected close to sample 39, show similar microfabrics and yield calcite/dolomite equilibration temperatures of  $370\text{--}380^\circ\text{C}$  (Table 2).

Sample 190 comes from the geometrically lowermost marble levels of the whole Alpi Apuane complex (Fig. 2). These marbles crop out in the core of a kilometric scale upright antiform (Fig. 6c), in which the main schistosity ( $D_1$ ) and all other  $D_1$ -structures are deformed by a later subhorizontal crenulation cleavage ( $D_2$ ). Sample 190

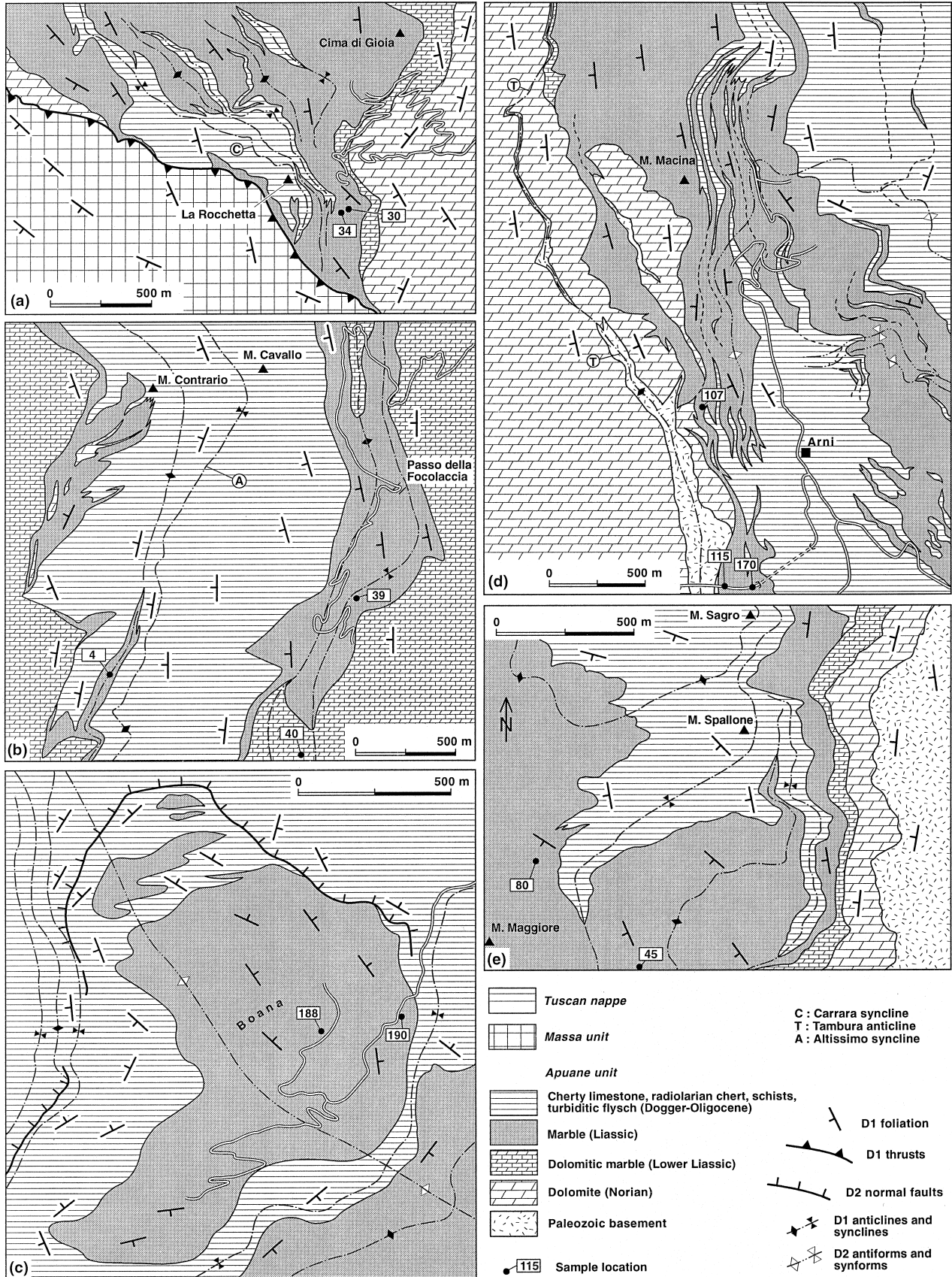


Fig. 6. Geological maps of the areas of samples locations (see Fig. 1 for the location of the maps). After Carmignani (1985), modified.

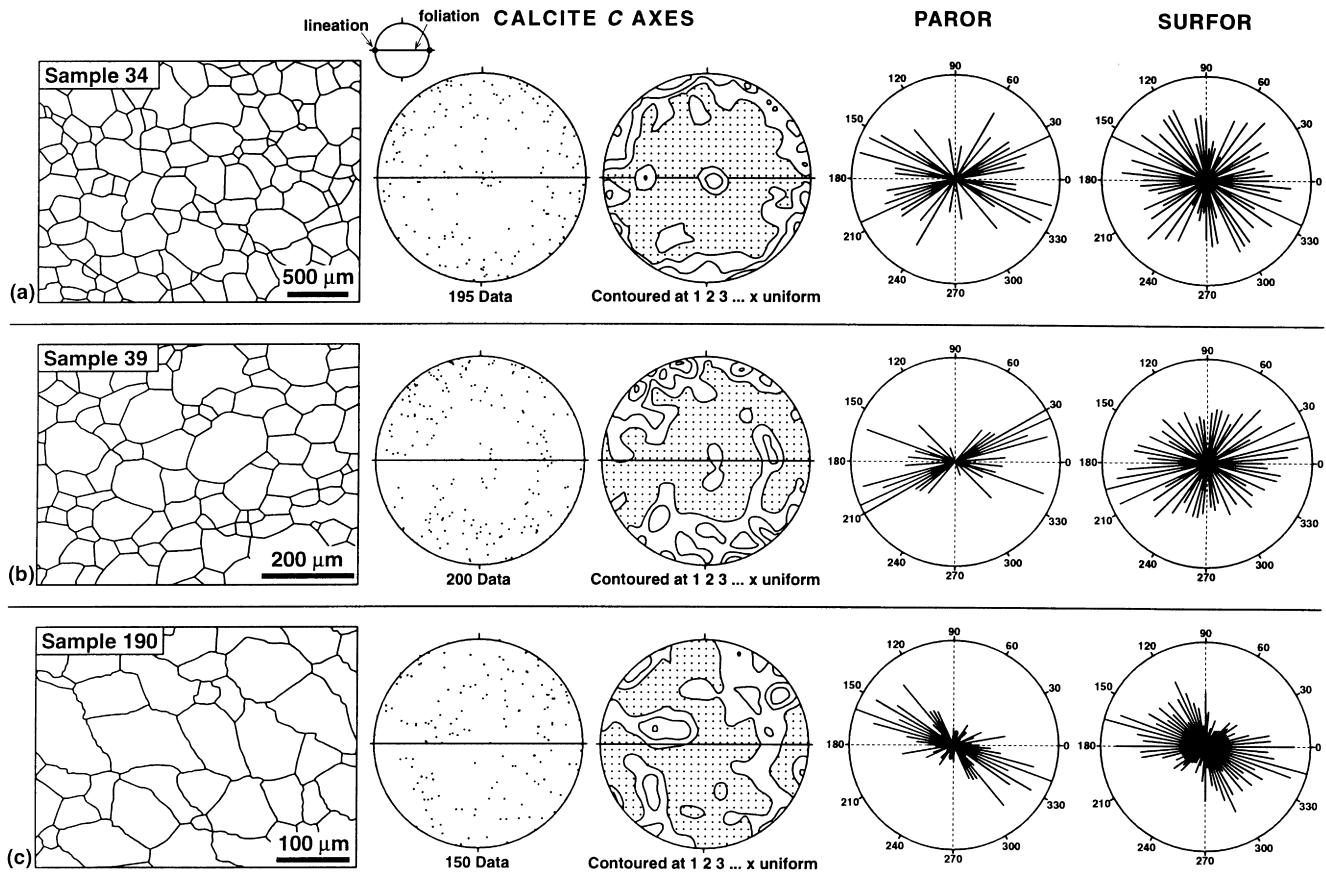


Fig. 7. Line-drawing of microstructures, *c*-axis orientation (from universal stage measurements) and results of PAROR and SURFOR analysis for calcite microfabric of samples 34, 39 and 190 (Type-A microfabric). Number of grains analysed with PAROR and SURFOR routines is more than 200.

shows an average grain size of about 100  $\mu\text{m}$  (Fig. 7c) and the analysis of the preferred orientation of grain boundary surfaces (SURFOR) reveals a nearly unimodal and asymmetrical surface orientation, showing a primary orientation at a low angle to the foliation trace. The analysis of the preferred orientation of particle axes (PAROR) shows a slightly bimodal distribution of long axis orientation, with the main maximum being inclined at approximately 20–30° with respect to the foliation plane, and a second maximum at

60°. Also in this sample the symmetry/asymmetry of the surface orientation and the preferred orientations of the particle axes coincide rather well. The average aspect ratios of the individual grains are in the order of 0.7 and the PARIS factor for the grain boundary geometry is around two. No clear preferred orientation of *c*-axis can be recognized. Calcite coexisting with dolomite in a sample collected nearby (sample 188, Fig. 6c, Table 2), indicates a maximum temperature of 360°C.

Table 3  
Results of microstructural analysis of representative samples of the different microfabric-types.

Sample	Microfabric type	Grain size ( $\mu\text{m}$ )	Grain size distribution	$\alpha^\circ$	PARIS	SPO	$T$ ( $^\circ\text{C}$ )
34	A	300	Unimodal	$\alpha_1 = 20^\circ \div 30^\circ$ $\alpha_2 = 20^\circ \div 30^\circ$	1.8	-	430 <sup>o*</sup>
39	A	90	Unimodal	$\alpha_1 = 20^\circ \div 30^\circ$ $\alpha_2 = 20^\circ \div 30^\circ$	2.3	-	370° ÷ 380 <sup>o*</sup>
190	A	100	Unimodal	$\alpha_1 = 20^\circ \div 30^\circ$	2	-	360 <sup>o*</sup>
170	B1	150 ÷ 200	Unimodal	$\alpha_1 = 10^\circ$	9	Parallel S1	390 <sup>o*</sup>
107	B2	Relict 150 Recryst. 40 ÷ 50	Bimodal	$\alpha_1 = 15^\circ$	Relict = 8 ÷ 15 Recryst. = 2 ÷ 3	Parallel S2	Relict = 400° Recryst. = 370°
45	B2	Relict 150 Recryst. 40 ÷ 50	Bimodal	$\alpha_{\text{relict}} = 15^\circ$ $\alpha_{\text{recryst.}} = 15^\circ$	Relict = 10 ÷ 23 Recryst. = 2 ÷ 3	Parallel shear Zone boundary	Relict = 420° Recryst. = 340°

\* Temperature of a nearby sample.

#### 4.2. Dynamically recrystallized microfabrics (type-B microfabrics)

Within type-B microfabrics two end-members of microstructures can be recognized: a) microstructures exhibiting strong shape preferred orientation, coarse grains and lobate grain boundaries (type-B1); b) microstructures with shape preferred orientation, smaller grain size and predominantly straight grain boundaries (type-B2). The two microstructures are quite different, but in a lot of samples lobate and straight grain boundaries occur at the same time. Samples showing type-B microfabrics are found in different structural positions in the nappe stack. In the following, we discuss sample 170 (type-B1 microfabric) and sample 107 (type-B2 microfabric) that come from the central Alpi Apuane, whereas sample 45 (type-B2 microfabric) comes from the western Alpi Apuane.

Sample 170 is derived from the highly sheared inverted limb of the kilometer-scale NE-facing  $D_1$  Tambura anticline (see profile in Figs. 2 and 6d). It shows coarse grain size, lobate grain boundaries, strong shape preferred orientation parallel to the main mesoscopic foliation, and a strong crystallographic preferred orientation (Fig. 8a). In mica-rich layers, pinning and window microstructures similar to that described by Jessell (1987) in quartzite are sometimes visible. Quantitative microstructural analysis (Fig. 9a) shows an average grain size of 150–200  $\mu\text{m}$  and a unimodal nearly symmetrical surface orientation with an orientation subparallel to the foliation trace. The analysis of the preferred orientation of particle axes (PAROR) shows a unimodal distribution of long axis orientation, with a maximum inclined at low angle approximately  $10^\circ$  with respect to the foliation plane. Individual grains are characterized by an average aspect ratio in the order of 0.50. A strong  $c$ -axis preferred orientation with a maximum normal to the foliation plane can be observed in this sample (Figs. 8b and 9a). Calcite/dolomite thermometry on sample 115, which was collected close to sample 170, shows the same microstructural features and indicates a temperature of about  $390^\circ\text{C}$  (Table 2).

Microstructure with straight grain boundaries (type-B2) is found in sample 107, that comes from the core of a kilometer-scale SW-verging  $D_2$  fold (Figs. 2 and 6d), refolding bedding and the  $D_1$  foliation ( $S_1$ ). This sample shows small recrystallized grains (40–50  $\mu\text{m}$ ), diffuse subgrains and core-mantle-like structures (Fig. 8c). Larger relict grains of the earlier microfabric are preserved. Quantitative analysis (Fig. 9b) shows preferred orientation of long axis particle orientation (PAROR) defining the foliation recognizable in thin section. Crystallographic preferred orientation shows a maximum of the  $c$ -axis at a low-angle and normal to the foliation plane (Fig. 9b). In contrast to the larger relict grains, which yield a calcite/dolomite equilibration temperature of about  $410^\circ\text{C}$  (sample 107A in Table 2), recrystallized grains are slightly zoned with Mg content, decreasing from

core to rim. Maximum temperatures calculated from the cores are about  $400^\circ\text{C}$  (sample 107Bc in Table 2); temperatures in the rims decrease to about  $370^\circ\text{C}$  (sample 107Br in Table 2).

Another kind of type-B microfabrics is found in sample 45, collected along mm- to dm-scale  $D_2$  shear zones (Fig. 8d–h), in the western Alpi Apuane (Figs. 2 and 6e). Approaching these shear zones, a gradual change in marble microfabric can be observed. In the low strain domains, the granoblastic protolith (mean grain diameter approximately 150  $\mu\text{m}$ ) shows type-A microfabric, even if low-temperature intracrystalline deformation (mainly undulatory extinction and deformation twins) can be observed. Towards the high strain zone (Fig. 9c), the grain boundary corrugation of the relict calcite, i.e. the PARIS factor, increases from about 10 to 23 (Table 3). Recrystallization occurs preferentially at the grain boundaries and a progressive localization of recrystallized grains in layers, subparallel to the shear zone boundaries, is observed (Fig. 8d). This transition is sketched in Fig. 10d. The recrystallized layers show a bimodal grain size distribution. Coarse, twinned relict grains (modal grain diameter about 200  $\mu\text{m}$ ) are embedded in a matrix of recrystallized grains with a diameter of approximately 40  $\mu\text{m}$  (Fig. 9d).

Sample 80, which shows the same microstructural type as sample 45, is characterized by a texture with  $c$ -axis small circle distribution oriented normal to the shear zone boundary (Fig. 8f). As illustrated in Fig. 8g, where recrystallized grains are masked, the few randomly distributed maxima can be related to the  $c$ -axis orientations of the relict grains. Due to bad sample statistics and a coarse grain size, a maximum of about 12 times uniform is obtained. The analysis of the completely recrystallized domain (Fig. 8h) of this type-B2 microfabric reveals that the  $c$ -axis orientations of the new grains are closely related to the relict  $c$ -axis orientations. Its small circle  $c$ -axis distribution is located in the same place as the maxima of the relict grains, shown in Fig. 8g. It is possible to interpret this feature as the result of a progressive reorientation of subgrains.

The calcite-dolomite thermometry applied in the fine-grained recrystallized calcite crystals of sample 45 yields maximum temperatures of about  $340^\circ\text{C}$  (sample 45B in Table 2). Granoblastic calcite grains in the low strain domains are zoned, showing Mg-rich cores and Mg-poorer rims. The maximum temperature calculated for the cores is  $390^\circ\text{C}$  (sample 45Ac in Table 2), whereas the Mg-content at the rim yields temperatures of  $360^\circ\text{C}$  (sample 45Ar in Table 2). Temperature distribution in these shear zones is sketched in Fig. 10d.

#### 4.3. Twinned microfabric (type-C microfabric)

The third type of microfabric is related to low-strain and low-temperature crystal plastic deformation mechanisms.

Characterized by thin straight  $e$ -twins (Fig. 10e), it occurs

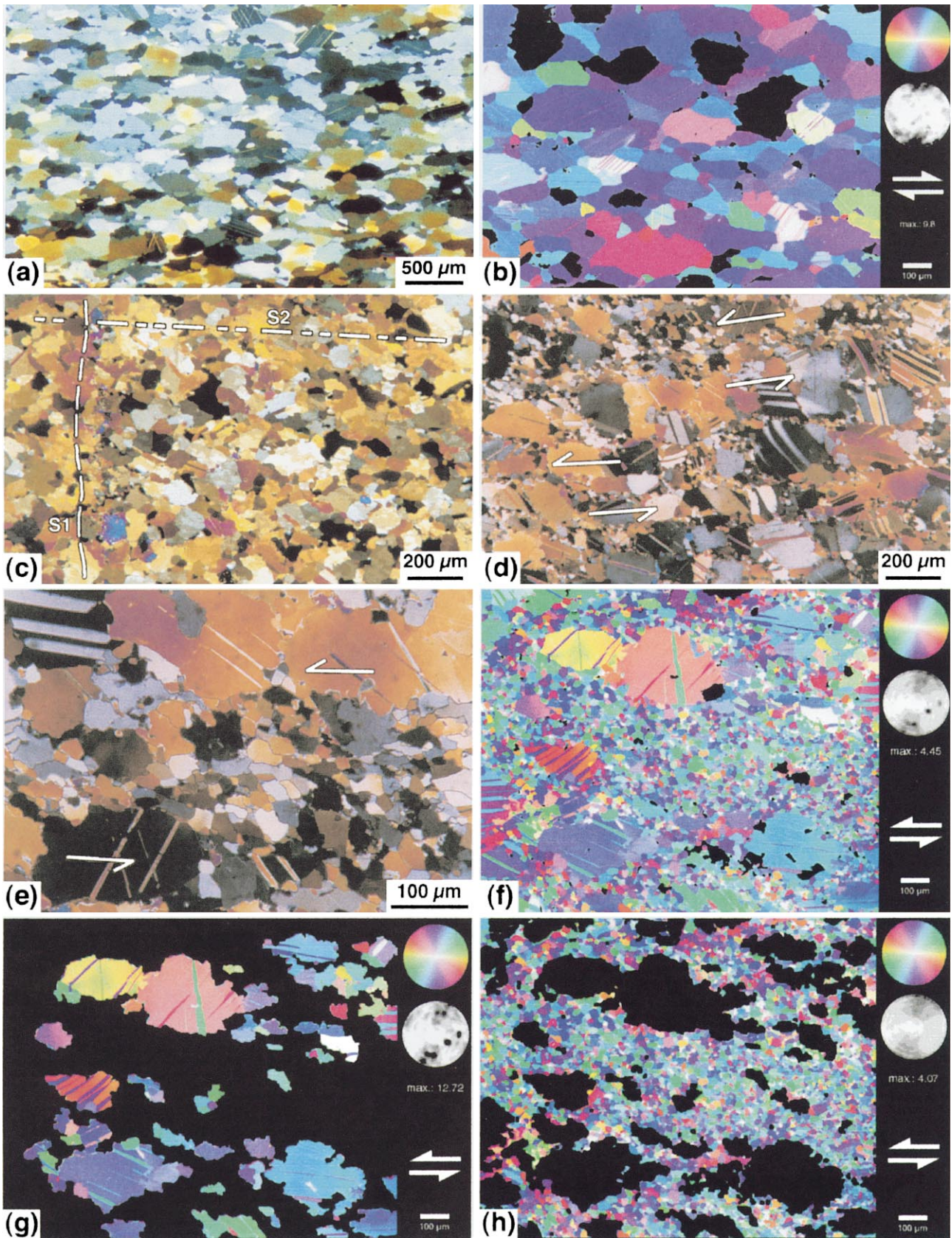


Fig. 8. Microstructures of dynamically recrystallized marbles. (a) Sample 170. (b) *c*-Axis orientations image (COI) revealed by CIP (Heilbronner Panozzo and Pauli, 1993) of sample 170. Strong *c*-axis maximum is located normal to the foliation plane. (c) Sample 107. (d) and (e) Sample 45. (f) COI of sample 80. (g) COI of relict grains in sample 80. Randomly distributed *c*-axis maxima can be related to single relict grains. (h) COI of recrystallized domain. The small circle *c*-axis maximum is located in the same place as the *c*-axis of the relict grains. Therefore subgrain rotation can be considered as the dominant recrystallization mechanism.

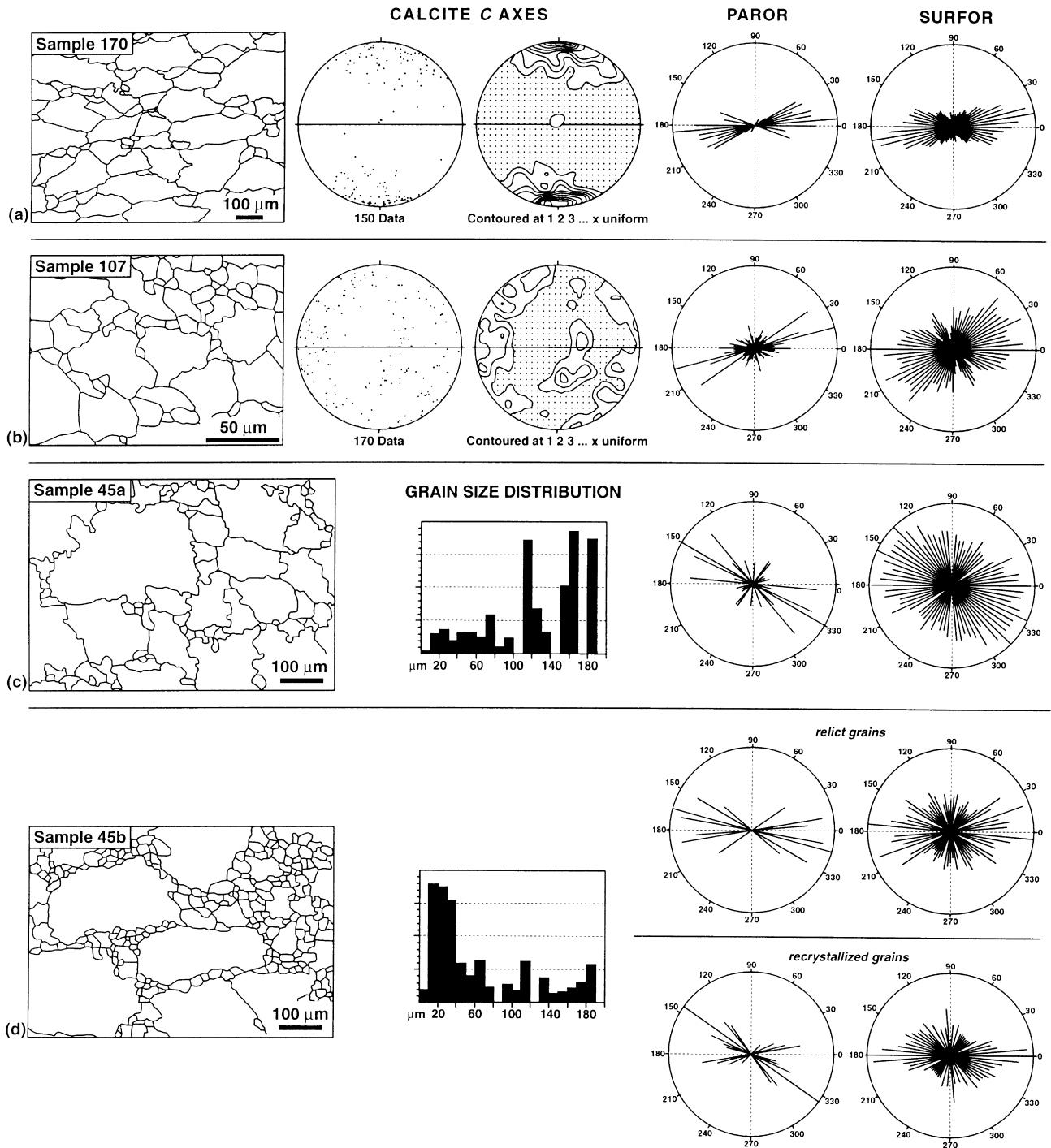


Fig. 9. Line-drawing of microstructures, *c*-axis orientation (from universal stage measurements) and results of PAROR and SURFOR analysis for calcite microfabric of samples 170, 107 and 45 (Type-B microfabric). For sample 45 grain size distribution, *c*-axis orientation for a similar microstructural type see sample 80 in Fig. 8f, g and h. Grain size distributions of samples 170, 107 and 45 (Type-B microfabric). Sample 45a shows an area with only limited reworking during  $D_2$ ; sample 45b shows an area that experienced more intense recrystallization during  $D_2$ . Number of grains analysed with PAROR and SURFOR routines is more than 200.

with different intensities in all the marble outcrops of the Alpi Apuane region, overprinting both type-A and type-B microfabrics.

It is well developed where large calcite grains are present.

In the case of type-B microstructures, where large and smaller grains are present (Fig. 8e), twinning affects only larger grains and not finer ones. This is in agreement with experimental studies indicating that twinning is easier in

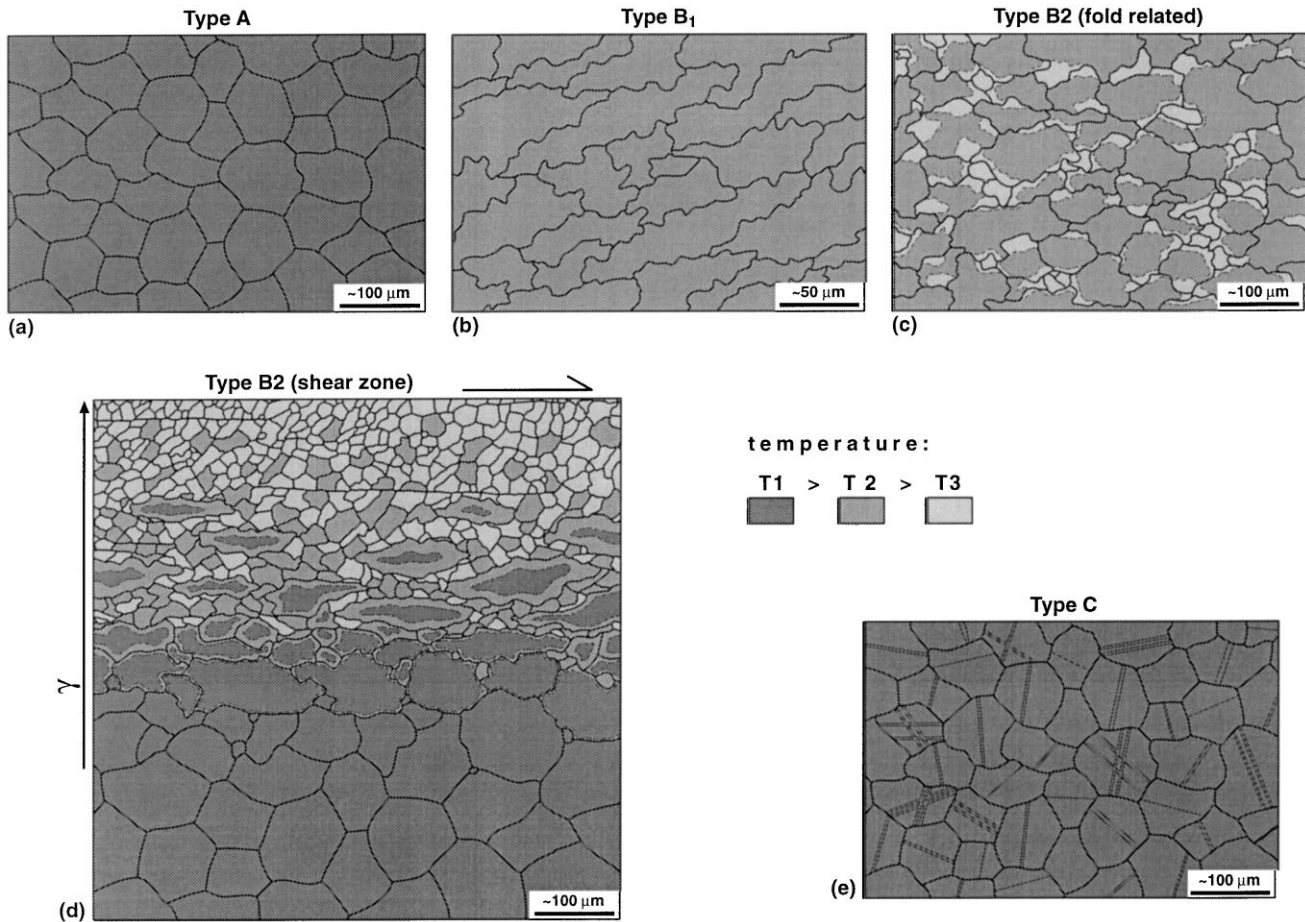


Fig. 10. Sketch showing the three types of microfabric described in this paper. (a) Type-A annealed microfabric. (b) Type-B1 dynamically recrystallized microfabric developed during late  $D_1$  deformation. (c) Type-B2 dynamically recrystallized microfabrics formed during folding. (d) Type-B2 dynamically recrystallized microfabrics formed along shear zone. Increasing strain is associated with grain size reduction. Different grey tones represent different calcite/dolomite temperatures ( $\gamma$  = strain). (e) Type-C twinned microfabric.

coarse grained than in fine grained-rocks, because the spreading and widening of twin lamellae are hampered by grain boundaries (Casey et al., 1978; Rowe and Rutter, 1990).

## 5. Carrara marble microfabrics and the tectonic evolution of the Alpi Apuane metamorphic complex: a discussion

### 5.1. Microfabric evolution and thermal history

The common microstructural features of samples 34, 39 and 190, such as the granoblastic polygonal grains with straight to slightly curved boundaries (very low PARIS factor ranging from 1.8 to 2.3), the unimodal grain size distribution, the absence of any optical evidence of internal strain and the weak or absent  $c$ -axis orientation, allowed us to interpret the type-A microfabric as developed during static recrystallization (annealing). This microstructure is sketched in Fig. 10a. The statically recrystallized micro-

fabrics are observable even though samples are collected in marble levels within kilometer-scale  $D_1$  isoclinal folds, where also minor parasitic folds developed. The presence of annealed microstructures within  $D_1$  folds (Fig. 5d) clearly indicates that the grain growth which produced type-A microfabric occurred after the main  $D_1$  folding phase, and obliterated all earlier syntectonic microstructures associated with folding. However, the presence of a weak texture in some samples can be possibly related to the pre-annealing deformation history.

The statically recrystallized marbles show an increase in grain size from the eastern to the western part of the Alpi Apuane complex, as already noticed by Zaccagna (1932) and Di Pisa et al. (1985). The latter authors interpreted the variation in grain size as related to a metamorphic paleo-gradient from the root zone (south west) to the front (north-east) during the  $D_1$  deformation affecting the metamorphic complex. The results of our thermometric studies confirm that the grain size variation in type-A microfabrics is associated with a temperature increase from east to west from 80–100  $\mu\text{m}$  and 360–380°C to 250–300  $\mu\text{m}$  and

420–430°C, but in our view static recrystallization occurred after main  $D_1$  folding. During static recrystallization history, one would expect that the structurally lower marbles experienced higher temperature than the structurally higher ones and should develop larger calcite grains. On the contrary, the composite cross sections of Fig. 2 show that coarse grained marbles of the western Alpi Apuane (samples 34–39) occur in a higher tectonic position with respect to the marbles of the central and eastern Alpi Apuane (sample 190). To explain this, we have to consider the tectonic evolution of the Alpi Apuane. If we restore the NE-directed transport of the late  $D_1$  phase, the higher portions of the nappe stack have to be located in a more westward and deeper position with respect to their present location. It is therefore more likely that annealing occurred at the time when the marbles of the western Alpi Apuane were in a deeper position than the marbles of the eastern Alpi Apuane.

The second type of microfabrics (type-B), characterized by: a) microstructures exhibiting coarse grains with lobate grain boundaries and strong shape preferred orientation (type-B1, sample 170, sketched in Fig. 10b); and b) microstructures with shape preferred orientation, smaller grain size and predominantly straight grain boundaries (type-B2, samples 45 and 107, sketched in Fig. 10c, d), are both interpreted as related to high strain and high temperature (350–400°C) crystal plastic deformation mechanisms (dislocation creep). Whereas grain boundary migration recrystallization can be considered as predominant in type-B1 microfabric, an important contribution of both rotation recrystallization and grain boundary migration can be inferred to prevail in type-B2 microfabric.

Sample 170, which shows a type-B1 microfabric, is characterised by a single  $c$ -axis maximum subperpendicular to the foliation plane (Figs. 8b and 9a). The interpretation of the texture-forming mechanism, quite common in naturally deformed marble, is still under discussion (Lafrance et al., 1994 and references therein). A similar texture was obtained in experimental deformation (Schmid et al., 1987), both in the twinning regime (where it is related to twin gliding and a substantial amount of  $r$ - and  $f$ -glide) and in grain boundary migration regime. The microstructural features of our sample point out that a comparison with the experimental grain boundaries migration regime appears more likely.

In samples 107 and 45 (type-B2 microfabric), syntectonic recrystallization of earlier large calcite grains is suggested by the presence of core-mantle structures, the progressive reorientation of subgrains  $c$ -axis, the polymodal grain size distribution, with larger relict grains associated with smaller new recrystallized ones, and by the wavelength of the grain boundary bulges that corresponds to the grain size of the newly formed recrystallized grains. We infer therefore that syntectonic recrystallization through rotation recrystallization and grain boundary migration postdate static recrystallization, i.e. type-B2 microfabrics overprint type-A microfabrics.

All type-B microfabrics show a shape preferred orienta-

tion of the grains which has allowed us to study the relationships between the development of such microstructures and meter- to kilometer-scale tectonic structures.

Sample 170 comes from a late  $D_1$  high strain zone (Tambura thrust) in the inverted limb of the Tambura anticline (Figs. 2 and 6d). The shape preferred orientation of grains is parallel to the main foliation recognizable in the field ( $S_1$ ) and refolded by the  $D_2$  folds. For this area, we therefore infer, that the development of type-B1 microfabrics is coeval with late  $D_1$  NE-directed transport along the inverted limb of the Tambura anticline.

Sample 107 comes from the core of a kilometer-scale SW-verging  $D_2$  fold (Figs. 2 and 6d), which refolds bedding and the  $D_1$  foliation ( $S_1$ ). The shape preferred orientation of the recrystallized grains is parallel to the mesoscopic axial-plane foliation ( $S_2$  in Fig. 8c) of  $D_2$  folds. This implies that  $D_2$  deformation can lead to crystal plasticity in marbles, too.

Late  $D_1$  and  $D_2$  deformations lead therefore to reworking of type-A microfabrics producing type-B microfabrics. These overprinting relationships are easily observable where  $S_1$  or  $S_2$  foliations are evident and type-B microfabrics develop a foliation recognizable at outcrop-scale. Nevertheless, most of the Alpi Apuane marbles are pure calcite marbles with no phyllosilicates or impurities, which mark a macroscopic foliation. In this case, it is difficult to determine if the dynamic microfabrics overprint an early annealed fabric or if they are related to earlier stages of  $D_1$  deformation surviving the static recrystallization and grain growth as proposed by Coli (1989). However, the investigated evolution of microstructures (sample 45) in pure marbles witnessing the transition from type-A to type-B microfabrics, points to the interpretation here proposed.

Analyses performed with the Dietrich and Song (1984) method on type-C microfabric (twinning) point out that in some samples where twinning is associated with type B-microfabrics, it is kinematically coherent with stress field related to the microfabric-producing event. In other samples, this relationship is not so straightforward, and it is difficult to demonstrate in the case of twinning affecting type-A microfabrics. Therefore, we suggest that at least a part of the twinning occurred at low temperature (minor than 200°C according to Ferril, 1991 and Burkhard, 1993), and has to be related to the most recent exhumation history of the metamorphic complex (cfr. Lacombe and Laurent, 1996).

## 5.2. Microfabric evolution and tectonic history

In the present study, the variability of statically and dynamically recrystallized microfabrics in the Liassic Alpi Apuane marbles has been emphasised. According to our microstructural observations the following evolutionary tectonic model can be proposed.

During the main regional deformation phase (early  $D_1$ , Fig. 11a), nappe emplacement, isoclinal folding producing

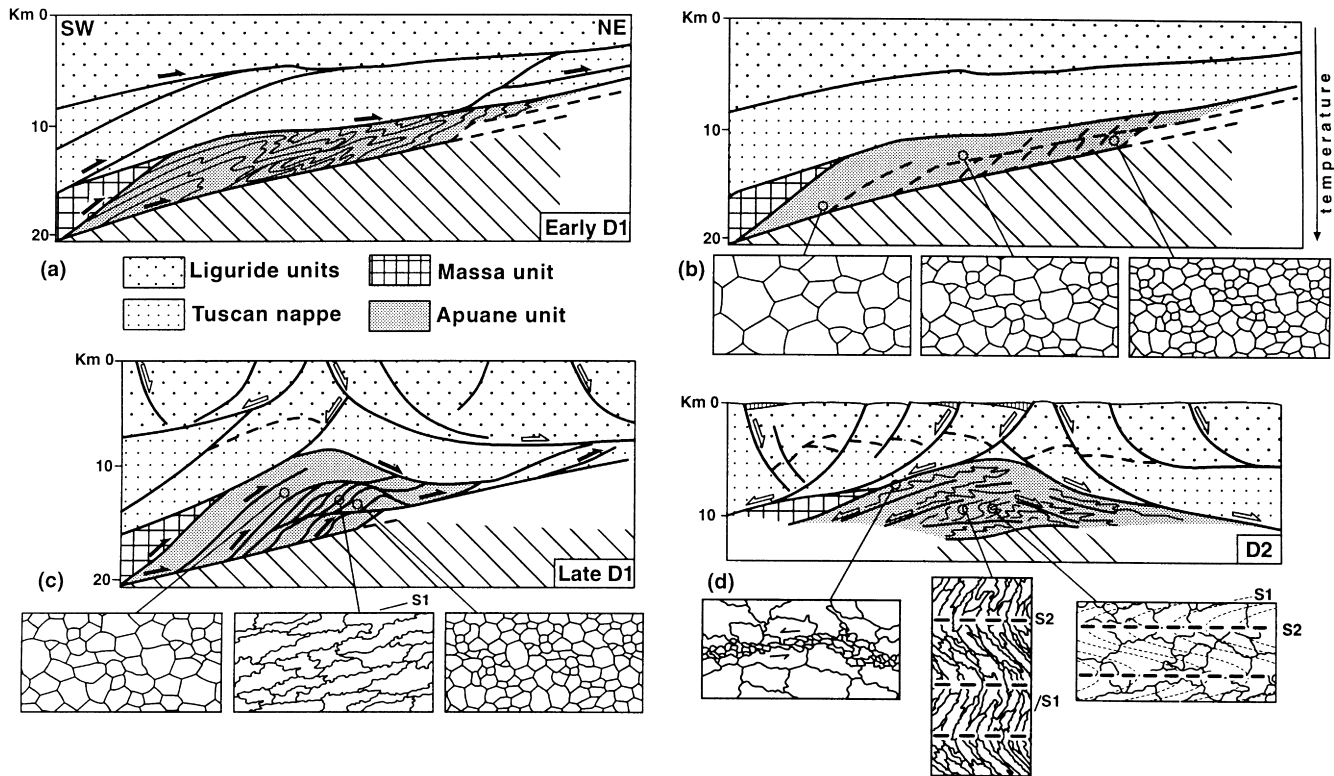


Fig. 11. Development of the Alpi Apuane structure (from Carmignani and Kligfield, 1990, modified) and marble microstructures. (a)  $D_1$  main folding phase, with top-NE nappe emplacement. During this phase main foliation and kilometer-scale isoclinal folds developed. (b) After  $D_1$  main folding phase annealing occurred, with complete obliteration of earlier microfabrics. In marbles polygonal granoblastic microstructures develop (type-A microfabrics). (c)  $D_1$  antiformal stack phase, with final NE transport along thrusts. Annealed microstructures are passively transported toward NE or reworked in shear zones along thrusts (type-B1 microfabrics). (d)  $D_2$  deformation leading to extension and exhumation.  $D_1$  features are folded or cut by later shear zones developed along low angle normal faults. Earlier microstructures can be reworked in  $D_2$  shear zones or along  $D_2$  fold axial planes (type-B2 microfabrics).

kilometer-scale NE-facing folds, stretching lineations and main foliation developed in the Apuane unit. After early  $D_1$  deformation (Fig. 11b), thermal relaxation and heating produced statically recrystallized fabrics (type-A microfabrics). The westernmost rocks were located in the deepest positions, and marbles developed the largest grain sizes and higher calcite/dolomite equilibrium temperature; easternmost marbles were in a higher position, and developed smaller grain sizes at lower temperature.

During the late stage of the  $D_1$  event (antiformal stack phase, Fig. 11c), further shortening was accomplished. In this phase, dynamic recrystallized microstructures (type-B1 microfabrics) were produced in localized, meter to decimeter-thick shear zones, where earlier type-A annealed fabrics were reworked. These shear zones accommodate the transport of the originally deeper westernmost tectonic levels toward NE in higher positions within the nappe stack.

The  $D_2$  history was associated with exhumation in retrograde metamorphic conditions (Fig. 11d). During this event, narrow millimeter- to decimeter-thick shear zones developed in the higher levels of the Alpi Apuane metamorphic complex (Carrara area), whereas folding occurred at lower levels (Arni area). The temperature was lower during  $D_2$  deformation than during  $D_1$ , but high enough to

produce syntectonic recrystallization (type B2 microfabric). This is testified by fine-grained calcite in  $D_2$  shear zones (sample 45), and recrystallized calcite grains elongated parallel to the axial surface of  $D_2$  folds (sample 107).

The difference in the temperature during the  $D_2$  event ( $380^\circ\text{C}$  in the east,  $340^\circ\text{C}$  in the west) can be related to the deeper position of rocks from the eastern area relative to rocks from the western area at the beginning of  $D_2$  deformation (Fig. 11d). This frame fits well with the different styles of  $D_2$  marble deformation, with predominant structures represented by large scale folding in the east as opposed to localized shear zones in the west. It is important to remember that not everywhere  $D_2$  folding produced dynamic recrystallization with shape preferred orientation tracing the axial plane of folding. In the case of open  $D_2$  folds, no significant reworking of earlier microstructures occurred, but only a passive reorientation of the previous microstructures.

Although the Carrara marble is widely used in experimental rock-deformation because of its nearly homogeneous fabric, with neither shape preferred orientation nor texture, our microfabric investigations at the scale of the whole Alpi Apuane area has pointed out a large variability of marble calcite microfabric originated during

static recrystallization as well as during various stages of the dynamic recrystallization which overprinted the “granoblastic” annealed fabric.

Presently running texture investigations on marbles at the scale of the whole Alpi Apuane region (Leiss and Molli, 1999; Oesterling et al., 1999; Rexin et al., 1999) will help to further develop the model of microfabric evolution and deformation history here presented.

## Acknowledgements

The authors want to acknowledge R. Heilbronner, H. Stünitz and L. Carmignani for the valuable suggestions. Many thanks are also due to E. Tavarnelli and B. Leiss for helpful and constructive reviews. G. Saviozzi is thanked for the ultra-thin section. Financial support from P.A.R. (Piano di Ateneo per la Ricerca) 1999—Prof. A. Larracotto is gratefully acknowledged.

## References

- Abbate, E., Balestrieri, M.L., Bigazzi, G., Norelli, P., Quercioli, C., 1994. Fission-track dating and recent rapid denudation in Northern Apennines, Italy. *Memorie della Società Geologica Italiana* 48, 579–585.
- Anovitz, L.M., Essene, E.J., 1987. Phase equilibria in the system  $\text{CaCO}_3\text{-MgCO}_3\text{-FeCO}_3$ . *Journal of Petrology* 28, 389–414.
- Bigazzi, G., Di Pisa, A., Gattiglio, M., Meccheri, M., Norelli, P., 1988. La struttura cataclastico-milonitica di Foce di Moschetta, Alpi Apuane sud-orientali (M. Corchia, Gruppo delle Panie). *Atti della Società Toscana di Scienze Naturali, Memorie, Serie A* 95, 105–116.
- Boccaletti, M., Gosso, G., 1980. Analisi della deformazione plicativa e rapporti con lo sviluppo della blastesi metamorfica nell’area di Campo Cecina-M. Pisanino delle Alpi Apuane settentrionali. *Memorie della Società Geologica Italiana* 21, 101–110.
- Bonatti, S., 1938. Studio petrografico delle Alpi Apuane. *Memorie Descrittive della Carta Geologica d’Italia* 26, 116.
- Burkhard, M., 1993. Calcite twins, their geometry, appearance and significance as stress and strain markers and indicators of tectonic regime: a review. *Journal of Structural Geology* 15, 351–368.
- Carmignani, L., 1985. Carta geologico-strutturale del Complesso Metamorfico delle Alpi Apuane, scala 125.000, Foglio nord. *Litografia Artistica Cartografica, Firenze*.
- Carmignani, L., Fantozzi, P.L., Giglia, G., Meccheri, M., 1993. Pieghie associate alla distensione duttile del Complesso Metamorfico Apuano. *Memorie della Società Geologica Italiana* 49, 99–124.
- Carmignani, L., Giglia, G., Kligfield, R., 1978. Structural evolution of the Apuane Alps; an example of continental margin deformation in the northern Apennines, Italy. *Journal of Geology* 86, 487–504.
- Carmignani, L., Kligfield, R., 1990. Crustal extension in the Northern Apennines: the transition from compression to extension in the Alpi Apuane core complex. *Tectonics* 9, 1275–1303.
- Casey, M.S., Rutter, E.H., Schmid, S.M., Siddans, A.W.B., Whalley, J.S., 1978. Texture development in experimentally deformed calcite rocks. In: Gottstein, G., Lücke, K. (Eds.), *Proceedings 5th International Conference on Textures of Materials*. Springer Verlag, pp. 231–240.
- Cerrina, F.A., Plesi, G., Fanelli, G., Leoni, L., Martinelli, P., 1983. Contributo alla conoscenza dei processi metamorfici di grado molto basso (anchimetamorfismo) a carico della falda toscana nell’area del ricoprimento apuano. *Bollettino della Società Geologica Italiana* 102, 269–280.
- Coli, M., 1989. Litho-structural assemblage and deformation history of “Carrara marble”. *Bollettino della Società Geologica Italiana* 108, 581–590.
- Coli, M., Fazzuoli, M., 1992. Considerazioni sulla litostratigrafia e sull’evoluzione sedimentaria delle formazioni retico-liassiche del nucleo metamorfico apuano. *Atti Ticinensi di Scienze della Terra* 35, 43–60.
- Covey-Crump, S.P., 1997. The high temperature static recovery and recrystallization behaviour of cold-worked Carrara marble. *Journal of Structural Geology* 19, 225–241.
- Crisci, G.M., Leoni, L., Sbrana, A., 1975. La formazione dei marmi delle Alpi Apuane (Toscana); studio petrografico, mineralogico e chimico. *Atti della Società Toscana di Scienze Naturali, Memorie, Serie A* 82, 199–236.
- D’Albissin, M., 1963. Les traces de la déformation dans les roches calcaires. *Revue de géogr. physique et de géologie dynamique (fascicule supplémentaire)*, 174 pp.
- De Bresser, J.H.P., 1991. Intracrystalline deformation of calcite. *Geologica ultraiectina* 79, 191.
- Dietrich, D., Song, H., 1984. Calcite fabrics in a natural shear environment. The Helvetic nappes of western Switzerland. *Journal of Structural Geology* 6, 19–32.
- Di Pisa, A., Franceschelli, M., Leoni, L., Meccheri, M., 1985. Regional variation of the metamorphic temperatures across the Tuscanid 1 Unit and its implications on the alpine metamorphism (Apuan Alps, N-Tuscany). *Neues Jahrbuch für Mineralogie, Abhandlungen* 151, 197–211.
- Di Sabatino, B., Giampalo, C., Potenza, P.L., 1977. Metamorfismo di “very low grade” ed altissima pressione nella “Unità delle Panie”. *Periodico di Mineralogia* 46, 79–89.
- Elter, P., 1975. Introduction à la géologie de l’Apennin septentrional. *Bulletin de la Société Géologique de France* 7, 956–962.
- Essene, E.J., 1982. Geologic thermometry and barometry. In: Ferry, J.M. (Ed.), *Characterization of Metamorphism Through Mineral Equilibria. Reviews in Mineralogy*, pp. 153–206.
- Essene, E.J., 1983. Solid solutions and solvi among metamorphic carbonates with applications to geologic thermobarometry. In: Reeder, R.J. (Ed.), *Carbonates: Mineralogy and Chemistry. Reviews in Mineralogy*, pp. 77–96.
- Essene, E.J., 1989. The current status of thermobarometry in metamorphic rocks. In: Daly, J.S., Cliff, R.A., Yardley, B.W.D. (Eds.), *Evolution of Metamorphic Belts. Geological Society of London Special Publications*, pp. 1–44.
- Ferril, D.A., 1991. Calcite twin widths and intensities as metamorphic indicators in natural low-temperature deformation of limestone. *Journal of Structural Geology* 13, 667–675.
- Franceschelli, M., Leoni, L., Memmi, M., Puxeddu, M., 1986. Regional distribution of Al-silicates and metamorphic zonation in the low-grade Verrucano metasediments from the Northern Apennines, Italy. *Journal of Metamorphic Geology* 4, 309–321.
- Franceschelli, M., Memmi, I., Carcangiu, G., Gianelli, G., 1997. Prograde and retrograde chloritoid zoning in low temperature metamorphism, Alpi Apuane, Italy. *Schweizerische Mineralogische und Petrographische Mitteilungen* 77, 41–50.
- Fredrich, J.T., Evans, B., Wong, T.F., 1989. Micromechanics of the brittle to plastic transition in Carrara Marble. *Journal of Geophysical Research* 94, 4129–4145.
- Giglia, G., Radicati di Brozolo, F., 1970. K/Ar age of metamorphism in the Apuane Alps (Northern Tuscany). *Bollettino della Società Geologica Italiana* 89, 485–497.
- Heilbronner Panozzo, P.R., Pauli, C., 1993. Integrated spatial and orientation analysis of quartz c-axis by computer-aided microscopy. *Journal of Structural Geology* 15, 369–382.
- Jessell, M.W., 1987. Grain boundary migration microstructures in a naturally deformed quartzite. *Journal of Structural Geology* 9, 1007–1014.
- Jolivet, L., Faccenna, C., Goffé, B., Mattei, M., Rossetti, F., Brunet, C., Storti, F., Funicello, R., Cadet, J.P., D’Agostino, N., Parra, T., 1998.

- Midcrustal shear zones in postorogenic extension: example from the northern Tyrrhenian Sea. *Journal of Geophysical Research* 103, 12123–12160.
- Kligfield, R., Hunziker, J., Dallmeyer, R.D., Schamel, S., 1986. Dating of deformation phases using K-Ar and  $40\text{Ar}/39\text{Ar}$  techniques; results from the Northern Apennines. *Journal of Structural Geology* 8, 781–798.
- Leiss, B., Molli, G., 1999. Natural “High Temperature” texture in Calcite from the Alpi Apuane, Italy. *Göttinger Arb. Geol. Paläont. SB4*, 100–101.
- Lacombe, O., Laurent, P., 1996. Determination of deviatoric stress tensors based on inversion of calcite data from experimentally deformed monophase samples: preliminary results. *Tectonophysics* 255, 189–202.
- Lafrance, B., White, J.C., Williams, P.F., 1994. Natural calcite c-axis fabrics: an alternative interpretation. *Tectonophysics* 229, 1–18.
- Mas, D.L., Crowley, P.D., 1996. The effect of second-phase particles on stable grain-size in regionally metamorphosed polyphase calcite marbles. *Journal of Metamorphic Geology* 14, 155–162.
- Molli, G., Giorgetti, G., 1999. Meso, microstructural and petrological constraints on the tectono-metamorphic evolution of the Alpi Apuane Complex (NW Tuscany, Italy). Exhumation of metamorphic terranes. *Rennes Meeting, Abstract volume*, pp. 54–55.
- Molli, G., Heilbronner, P.R., 1999. Microstructures associated with static and dynamic recrystallization of Carrara marble (Alpi Apuane, NW Tuscany Italy). *Geologie en Mijnbouw* 78, 119–126.
- Olgaard, D.L., Evans, B., 1988. Grain growth in synthetic marbles with added mica and water. *Contributions to Mineralogy and Petrology* 100, 246–260.
- Oesterling, N., Heilbronner, R., Molli, G., 1999. Textures of Calcite-Mylonites in Carrara Marble. Comparison of Computer Integrated Polarization Microscopy (CIP) and Universal Stage-Measurements. *Göttinger Arb. Geol. Paläont. SB4*, 144–145.
- Panozzo, R., 1983. Two-dimensional analysis of shape fabric using projection of lines in a plane. *Tectonophysics* 95, 279–294.
- Panozzo, R., 1984. Two-dimensional strain from the orientation of lines in a plane. *Journal of Structural Geology* 6, 215–221.
- Panozzo, R., Hürlimann, H., 1983. A simple method for the quantitative discrimination of convex and convex-concave lines. *Microscopica Acta* 87, 169–176.
- Rexin, E., Leiss, B., Molli, G., 1999. Microstructures and textures of the Carrara Syncline, Alpi Apuane Italy. *Göttinger Arb. Geol. Paläont. SB4*, 163–164.
- Reutter, K., Teichmüller, M., Teichmüller, R., Zanzucchi, G., 1983. The coalification pattern in the Northern Apennines and its paleogeothermic and tectonic significance. *Geologische Rundschau* 72, 861–894.
- Rowe, K.J., Rutter, E.H., 1990. Paleostress estimation using calcite twinning: experimental calibration and application to nature. *Journal of Structural Geology* 12, 1–17.
- Rutter, E.H., 1972. The influence of interstitial water on the rheological behaviour of calcite rocks. *Tectonophysics* 14, 13–33.
- Rutter, E.H., 1995. Experimental study of the influence of stress, temperature, and strain on the dynamic recrystallization of Carrara marble. *Journal of Geophysical Research* 100, 24651–24663.
- Sander, B., 1950. Einführung in die Gefügekunde der geologischen Körper, zweiter Teil: Die Korngefüge. Springer, Wien.
- Schmid, S.M., Panozzo, R., Bauer, S., 1987. Simple shear experiments on calcite rocks: rheology and microfabric. *Journal of Structural Geology* 9, 747–778.
- Schmid, S.M., Paterson, M.S., Boland, J.N., 1980. High temperature flow and dynamic recrystallization in Carrara marble. *Tectonophysics* 65, 245–280.
- Schultz, H., 1996. Analyse der variszisch-äpeninischen Deformationsgeschichte des paläozoischen Basements der Apuaner Alpen (Toskana, Italien), *Berliner Geowissenschaftliche Abhandlungen. Reihe A: Geologie und Paläontologie* 188, 108.
- Spiers, C.J., 1979. Fabric development in calcite polycrystals deformed at 400°C. *Bulletin de Minéralogie* 102, 282–289.
- Storti, F., 1995. Tectonics of the Punta Bianca promontory: Insights for the evolution of the Northern Apennines-Northern Tyrrhenian Sea basin. *Tectonics* 14, 832–847.
- Wenk, H.-R., Takeshita, T., Bechler, E., Erskine, B.G., Matthies, S., 1987. Pure shear and simple shear calcite textures. Comparison of experimental, theoretical and natural data. *Journal of Structural Geology* 9, 731–745.
- Zaccagna, D., 1932. Descrizione Geologica delle Alpi Apuane. *Memorie Descrittive della Carta Geologica d’Italia* 25, 440.